Computers & Geosciences 86 (2016) 23–33

Contents lists available at ScienceDirect

Computers & Geosciences

journal homepage: www.elsevier.com/locate/cageo

Case study

Neuro-evolutionary event detection technique for downhole microseismic surveys

Debotyam Maity *, Iraj Salehi

Gas Technology Institute, 1700 S. Mount Prospect Road, Des Plaines, IL 60018, USA

ARTICLE INFO

Article history:
Received 12 March 2015
Received in revised form
14 July 2015
Accepted 30 September 2015
Available online 8 October 2015

Keywords:
Downhole microseismic
Hydraulic fracturing
Event detection
Neural network
Evolutionary algorithm
Autopicking

ABSTRACT

Recent years have seen a significant increase in borehole microseismic data acquisition programs associated with unconventional reservoir developments such as hydraulic fracturing programs for shale oil and gas. The data so acquired is used for hydraulic fracture monitoring and diagnostics and therefore, the quality of the data in terms of resolution and accuracy has a significant impact on its value to the industry. Borehole microseismic data acquired in such environments typically suffer from propagation effects due to the presence of thin interbedded shale layers as well as noise and interference effects. Moreover, acquisition geometry has significant impact on detectability across portions of the sensor array. Our work focuses on developing robust first arrival detection and pick selection workflow for both P and S waves specifically designed for such environments. We introduce a novel workflow for refinement of picks with immunity towards significant noise artifacts and applicability over data with very low signal-to-noise ratio provided some accurate picks have already been made. This workflow utilizes multi-step hybrid detection and classification routine which makes use of a neural network based autopicker for initial picking and an evolutionary algorithm for pick refinement. We highlight the results from an actual field case study including multiple examples demonstrating immunity towards noise and compare the effectiveness of the workflow with two contemporary autopicking routines without the application of the shared detection/refinement procedure. Finally, we use a windowed waveform cross-correlation based uncertainty estimation method for potential quality control purposes. While the workflow was developed to work with the neural network based autopicker, it can be used with any other traditional autopicker and provides significant improvements in pick detection across seismic gathers.

1. Introduction

Microseismic monitoring has become an integral part of most unconventional resource development programs. They have found wide utility in reservoir monitoring as well as resource characterization studies. Phase arrival information is critical in identifying other microseismic source parameters of relevance such as event size and hypocentral location. One of the most common algorithms for detection is the short term averaging/long term averaging (sta/lta) algorithm (Allen, 1978). Methods based on abrupt changes in attributes of the seismic waveform such as higher order statistics (skewness and kurtosis by Saragiotis et al. (2002)) have also been used. Modern autopickers can use advanced techniques such as cross-correlation analysis (Song et al., 2010), polarization obtained from signal covariance matrix (Fischer et al., 2007), parallelized filters (Lomax et al., 2012), Bayesian probabilistic approach for concurrent events (Wu et al., 2015), singular value decomposition of 3-C seismograms (Kurzon et al., 2014) and robust statistical techniques (Chen, 2005). Noise artifacts can cause autopicker efficacy to gradually degrade though the effect of different types of noise on different autopickers can vary significantly. For downhole sensor deployments, the quality of the first arrival pick is related to sub-surface structure (such as velocity contrasts and layering), source type, source–receiver geometry, and finally, downhole noise conditions. These factors can lead to complicated wave-trains (such as head waves and reflections) and require human intervention to prevent miss-picks. Finding a robust methodology to work under extreme noise conditions is therefore a significant challenge.

In this article we use a robust hybrid neural network autopicker (Maity et al., 2014) to make initial pick estimates. Then we use an evolutionary algorithm to make the best possible arrival detection based on the initial pick estimates. The basic assumption behind the suggested approach is that moveout behavior of direct arrivals

* Corresponding author.
E-mail addresses: Debotyam.Maity@gastechnology.org (D. Maity), Iraj.Salehi@gastechnology.org (I. Salehi).

http://dx.doi.org/10.1016/j.cageo.2015.09.024
0098-3004/

is predictable as it is hyperbolic and can be approximated using a high order polynomial function. The algorithm has been extensively tested on real microseismic monitoring data from multiple gas well completions in the Marcellus shale reservoir and the results have been compared with contemporary autopickers in use by the industry to validate, both qualitatively and quantitatively, the applicability of our proposed approach. The use of genetic algorithms allows for optimized search and rapid detectability even for extremely large gathers (hundreds of data channels).

2. Method

2.1. Neural network based autopicking algorithm

A robust neural network based autopicking approach is used to make initial pick estimates. Maity et al. (2014) provide a detailed understanding of the autopicking workflow used for this study and can be used as a reference. In brief, the workflow involves preprocessing steps such as noise removal through application of frequency filters, data rotation to maximize phase arrival energy on corresponding components, etc. For selection of training, validation and testing data subsets, a careful selection procedure is used to account for various arrival artifacts ranging over significant spread of the energy and frequency spectrums of the dataset being processed. For network input design, multiple seismic data attributes are evaluated (such as wavelet transform, statistical measures, or others from available autopicker algorithms, etc.). Data subset selection involves careful analysis of the filtered spectrum and identifying phase types of interest and making sure that the corresponding phase arrivals are picked up with reasonable accuracy by some, if not all of the selected data attributes. At the same time, various incoherent noise artifacts are also selected within the data subsets for improved training of network models as classifiers. In short, representative training dataset should include interference, reflection, refraction and other propagation and noise effects that are typically observed in downhole microseismic survey datasets being studied. Next, any redundant attributes are identified and pruned by correlation of normalized and rescaled attribute measures. The aim is to minimize the number of attributes to be used in the training process to reduce run times and to increase the accuracy without dilution in results due to too many attributes or by having a non-representative model due to too few attributes. A neural network is used to map the input attributes to an output characteristic function which has highs of 1's at the phase onsets and 0's otherwise. The data subset selected is subdivided into training, validation and testing sets using statistical measures such as mean and skewness of distribution to verify representativeness. The nodal inputs to the network are defined by the selected attributes. The hidden layer is designed based on the number of input and output layer nodes. An evolutionary algorithm is used for network optimization. The output characteristic function as obtained by applying the trained network on any dataset is used for pick selection as required and we will call this function as AP1 for future reference.

2.2. Contemporary picking algorithms

Two contemporary autopicking algorithms were tested in a comparative framework along with the proposed hybrid AP2 workflow in order to test and benchmark its performance. The first method used is the FilterPicker algorithm which involves multiple filters operating in parallel. The final picker characteristic function is calculated as the envelope from a derived function which combines the results from each filter. Lomax et al. (2012) provide a very detailed understanding of the FilterPicker workflow. The other picking algorithm used is the standard "sta/lta" averaging method as implemented within microseismic monitoring (MIMO) package developed by NORSAR. The signal detections or first break picks are made based on signal-to-noise ratio crossing predefined threshold and falling back below threshold within a reasonable time interval. Oye and Roth (2003) provide a detailed understanding of the picking and phase detection algorithm used within MIMO package. In this study, errors generated by the processing packages were disregarded and actual time offsets based on comparisons with manual picks were used for evaluation.

2.3. Pick refinement

Based on the output map obtained from any of the mentioned picking workflow, we expect higher values of characteristic function to be indicative of possible pick locations and vice versa. The picking approach involves time averaging of the autopicker characteristic function before using limiting thresholds predefined by the user. As the average moves beyond the defined threshold, a possible pick is declared and then a check is made to ensure that the time averaged value of the characteristic function falls below the defined threshold before a second pick can be considered. Once a pick is declared, the algorithm selects the peak (local maxima) on the picker characteristic function as potential pick location within the defined pick window (as obtained based on when the value of the time averaged characteristic function rises above and falls below predefined thresholds). A quality control mechanism can be used which checks for ratio of two statistical measures (mean and maximum) across the pick within the identified pick window and picks are quality controlled based on these ratios.

2.4. Evolutionary search for optimal pick across gathers

Before final detection using evolutionary search, misclassified picks can be removed if necessary using a weighted pick density criteria which is evaluated for each pick. This criteria and its use is based on the fact that for borehole geophone strings, the moveout is generally smooth across the gather for seismic events. This indicates that if a pick is located accurately on an individual trace across a seismic gather, it should be straddled with other picks as we move along the gather due to proximity of geophones compared with typical travel paths. The density measure is computed for *i*th trace by using a weighted summation approach along each pick within a predefined evaluation window as shown in Eq. (1).

$$\tau_P(i) = \sum_{j=i-N_t}^{i+N_t} \sum_{k=\tau(j)-win}^{\tau(j)+win} AP1_{j,k} \tag{1}$$

Here, N_t defines the number of traces close to the evaluation trace for calculation which can even include all traces across gather when looking for far-field events. The variable k allows for summation over a predefined window size where presence of other picks increases pick density. This measure is normalized based on the observed maximum and minimum over all picks made using AP1 characteristic function. Finally, the picks associated with the lower *n*th percentile of the density distribution are pruned as erroneous provided the evaluated signal-to-noise ratio taken cumulatively for all traces is reasonably low. Fig. 1 shows a sample gather with the initial picks and the final pruned picks using this measure. For this study, we use a cutoff at 10th quantile, i.e., any pick location with a probability falling below the 10th quantile of associated probability function is removed.

With the picks from the refinement step available for analysis, evolutionary search can be applied to detect events across gather. As indicated earlier, this technique is only applicable for borehole

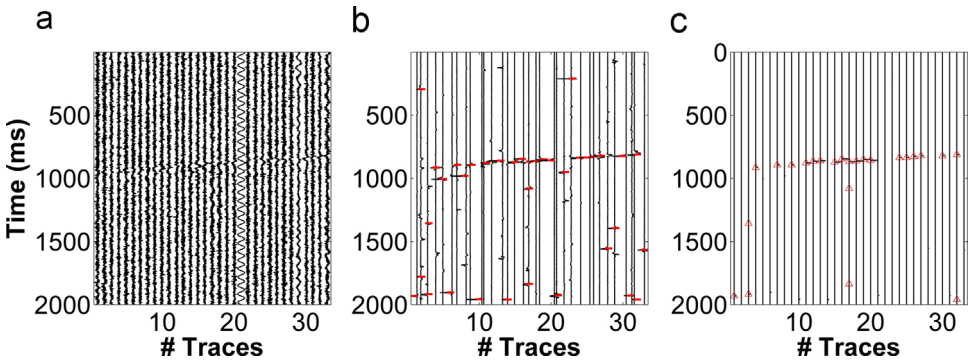

Fig. 1. Subplot (a) shows recorded gather without any processing, (b) shows AP1 output (picker characteristic function) and preliminary picks while (c) shows pick probability map and refined picks. Red inserts show pick location for subplots (b) & (c). (For interpretation of the references to color in this figure legend, the reader is referred to the web version of this article.)

data or with surface data where moveout behavior can be approximated by a high order polynomial function. We use a genetic algorithm which mimics the theory of evolution by natural selection wherein the less fit individuals from each generation are selectively eliminated before a new generation is created. This selection is an iterative process where an objective function is used to evaluate the fitness of each individual in the population and new generations are obtained by probabilistically selecting fitter individuals from current generation. The fitness function is a weighted summation of individual functions relating to minimizing the mean squared error based on the misfit for each pick (Eq. (2)) as well as number of qualified "good picks" identified as those relatively close to the polynomial fit (Eq. (3)). This closeness is evaluated based on the quality of each pick (the local maximum of the AP1 characteristic function) and the Euclidean distance between the AP1 pick and polynomial fit value. Function "τ" is the final optimization function to be minimized (Eq. (4)).

$$\theta(x) = 1/\sum_{i=1}^{\text{no. of traces}} \left[AP1\_pick_i - fit\_value_i\right]^2 \tag{2}$$

$$\phi(x) = 1/[\#\text{good picks}] \tag{3}$$

$$\tau(x) = 1/[\phi(x) \times \theta(x)] \tag{4}$$

Beyond these optimization functions, certain hard constraints on fitting can also be used including the concave down condition based on the survey geometry and a constraint of maximum moveout (fit curvature) based on the expected source–receiver separations which also helps remove those far field events (such as noise artifacts) not associated with the actual hydraulic fracturing treatment. Some members of the parent population are also subjected to genetic operators such as cross-over and mutation to generate new offspring. In short, the fitness function used tries to identify the best possible polynomial fit through the initial picks available provided the error in mismatch is reduced but at the same time, better picks (as per quality of the initial picks) are more heavily weighted through higher scoring of the individuals. A probability measure is used to decide on the percentage of individuals from parent population that will be copied (while the rest undergo cross-over). This probabilistic selection is implemented through a rank selection process where the probability of selection of individual is inversely proportional to its position in the sorted population list based on fitness. Once selection of the crossover candidates is made, the operation involves a random subpart from the parent pair being swapped to generate two offspring pairs. A uniform crossover technique is used for this study. Finally, a relatively small portion of the offspring population is chosen at random and a randomly selected bit is flipped in the selected population set to generate mutated offspring. In order to reduce crowding effects (where similar individuals crowd a population set), fitness sharing strategy is implemented which rescales the evaluated fitness based on the number of similar individuals in a population. The entire workflow involving initial picking followed by evolutionary search for best pick has been described in Fig. 2 for reference.

We also measure uncertainty in arrivals by assuming each pick to be accurate and estimating the location of the best pick along other traces with the assumption that the waveforms for all traces at arrival should be similar. This sliding window cross-correlation analysis method allows isolating events with high uncertainty observed as wider spread of cross-correlation maximums. Fig. 3 shows two sample traces with high/low noise artifacts leading to higher/lower arrival uncertainty as measured with all other traces within the event gather.

Uncertainty estimates are influenced not just by the quantum of noise observed within each gather, but also on the lack of distinct arrivals due to the characteristics of the source as well as the structural properties of the medium and their impact on seismic wave propagation. As an example, consider a simple synthetic test case where a double couple source aligned in X–Z direction (Fig. 4a) shows energy release wherein much of the compressional wavefront does not reach the geophones (Fig. 4b–d) due to the source–receiver geometry specified for this case. Geologic features such as layer boundaries with very high impedance contrasts or significant anisotropy can also impact observed energy arrivals and consequently, the associated pick uncertainties. As an example, depending on the layer velocities in question and the source–receiver geometry, head waves become possible which in turn can interfere with P wave arrivals and add to uncertainty. Similarly layer boundary reflections can interfere with S wave arrivals and add to uncertainty.

In this study, a thorough analysis of this observed uncertainty and its impact on further processing steps has not been undertaken. We believe that when travel time inversion algorithms are used to identify source parameters using phase arrival data, those geophones showing significant uncertainty have to be omitted.

3. Case study

Let us consider a sample event detection of relatively high signal-to-noise ratio (approximately 10) data and understand the results from the detection workflow as observed.

Based on the initial picking algorithm (AP1), picks are made across the gather as observed in Fig. 5. We note that each trace is assigned a unique pick based on the maxima observed with the AP1 characteristic function (Fig. 5c). This can be modified to allow

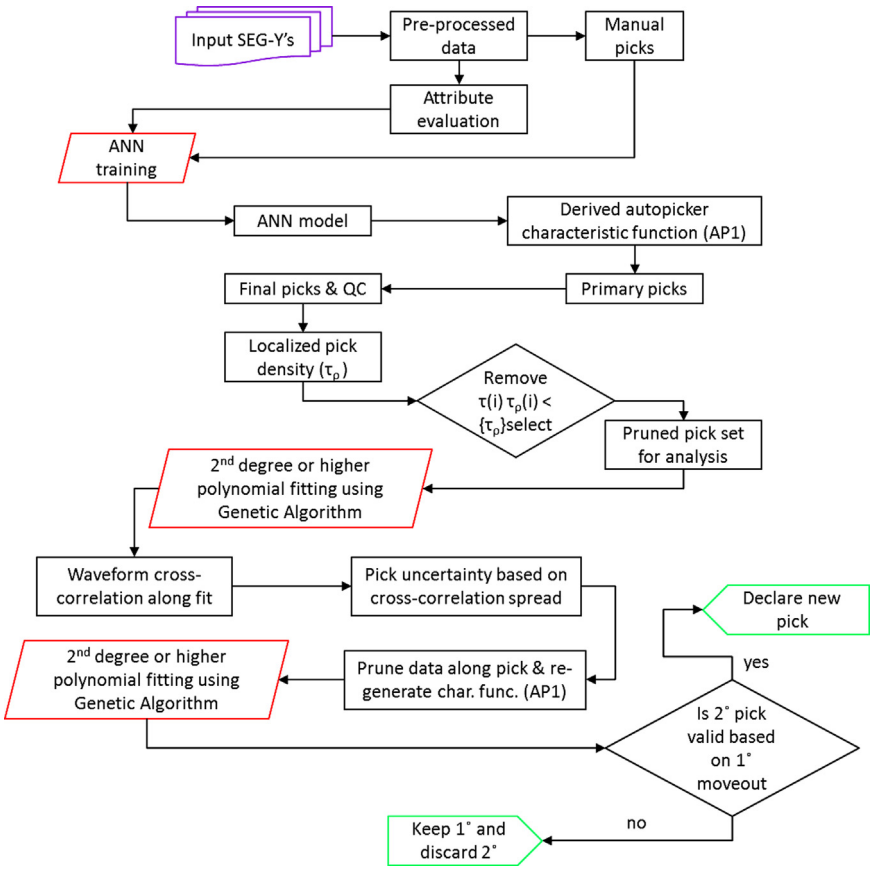

Fig. 2. Initial picking and event detection workflow for datasets with predictable moveout.

for multiple picks along each trace based on AP1 derived characteristic function's local behavior. We also note that this event has multiple phase arrivals which could be a result of two temporally separate events (by approximately 0.6 s).

Based on the initial picks identified by AP1, an initial fit is obtained so as to randomly fit all of the identified picks (Fig. 6a). The polynomial fitting routine using an evolutionary algorithm for optimization is run so as to minimize the objective function. Parameters used for both the AP1 and AP2 workflows in this case study are specified in Table 1.

The final pick location is selected based on local maxima in AP1 characteristic function close to the final identified polynomial fit and the pick uncertainty is defined based on a secondary cross correlation analysis close to the identified picks across the gather. Fig. 6b depicts the optimization process for the sample event with the iterative search process to identify the optimal pick.

Once the primary pick has been identified, the workflow reruns the AP1 algorithm for segmented data sections before and after

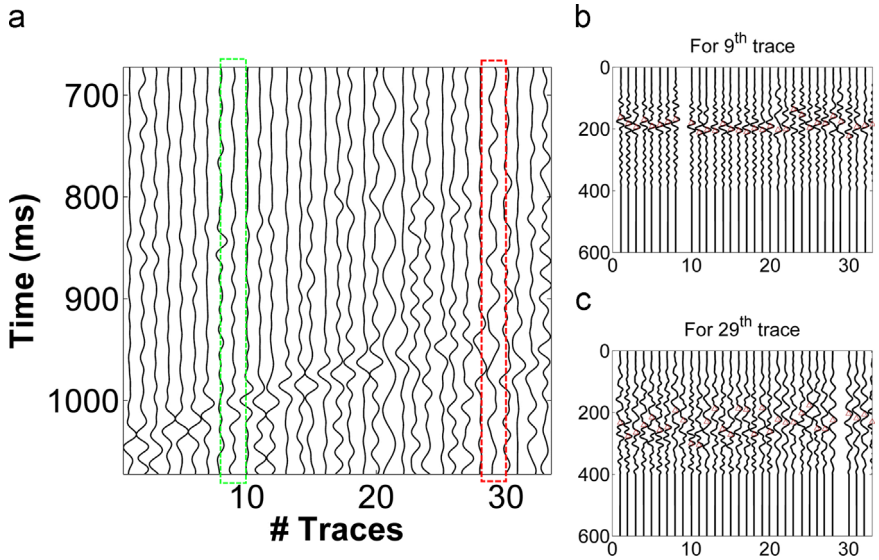

Fig. 3. Subplot (a) shows a sample gather with a relatively noisy (29th) and a relatively noise free (9th) trace. Subplots (b) and (c) show cross-correlation results with other traces within gather at arrival for 9th and 29th trace.

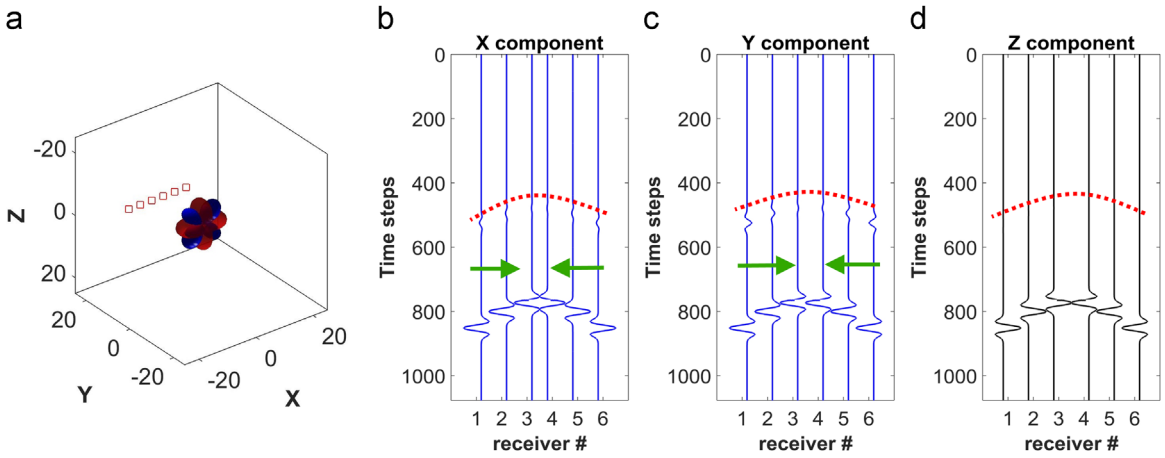

Fig. 4. Sample synthetic test case showing (a) source–receiver geometry with 6 subsurface receivers and a double couple source with (b), (c) and (d) showing synthetic 3C data generated highlighting very low compressional wave energy at arrivals. Dotted inserts in (b) highlight expected P-wave arrivals and arrows indicate direction of increasing uncertainty for P-wave arrival.

the identified pick to detect secondary arrivals. In case an arrival is detected before the first pick onset, the primary is classified as S phase pick and the new secondary detection is classified as P phase pick. Fig. 7 shows the initial estimate using the segmented dataset and the iterative search process leading to optimal secondary detection. Both primary and secondary fits seem to be more or less linear with the primary showing a smaller slope (~ -8) compared with the secondary pick (~ -5.7). This is expected since the primary pick is actually the S phase onset which should show a higher slope due to slower shear wave velocity. Moreover, the primary pick shows a higher intercept constant (arrival at 1st trace) compared to the secondary pick as expected.

The final picks (primary S phase and secondary P phase detection) are shown in Fig. 8. We observe relatively accurate P and S phase arrival detection with maximum absolute error in arrival observed as approximately 24 ms and the average error in arrival observed at approximately 7 ms. This seems reasonable for an automated picking workflow which does not include any post-detection pick refinement and also does not try for any significant noise reduction prior to picking. However, the sample event shared has relatively high signal-to-noise ratio and the results should degrade with increased noise.

Looking at the uncertainty estimates for both P and S phase arrivals made for the sample event trigger (Fig. 9), we observe high uncertainty for picks on traces 21 and 29 for primary and for picks on traces 21, 27 and 29 for secondary detection. This uncertainty is highlighted through the trace display (Fig. 10) which includes the original picks made using the AP1 picker. Trace 21 is observed to be instrument noise, trace 27 has relatively small first break arrival energy and trace 29 has low frequency noise artifact causing high pick uncertainty.

Based on the uncertainty estimates and the percentage of uncertain picks classified per event detected, a picked event is declared for comparative analysis.

4. Results

While the case study discussed highlights a single event file with relatively high signal-to-noise ratio, the strength of this methodology lies in its ability to isolate hard to detect noisy microseisms. This workflow was applied on monitoring data from multiple hydraulic fracturing stages (>18) from a few Marcellus gas wells. In this discussion, we limit ourselves to a very small subset (20 event trigger files with a total of 660 traces) of this large dataset for a comprehensive analysis involving visual inspection and manual phase picking as well as comparisons with available open source contemporary event detection algorithms. Of these 20 files, we share 4 event files in this article to highlight the robustness of this detection workflow. Fig. 11 shows four sample event files from this data subset under study and we can clearly see events with moderate to very low signal-to-noise ratios for P phase onset, wave reflection/interference artifacts as well as potential survey geometry related artifacts. These events depict typical microseismic detections in borehole environments where poor instrument clamping causes low signal strength and potential borehole noise artifacts.

The same workflow as discussed under the case study is

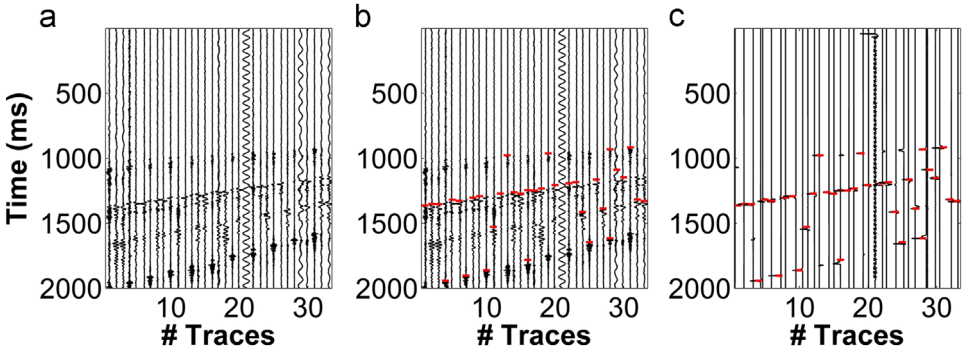

Fig. 5. Sample event file showing multiple arrivals with subplot (a) showing original data, (b) showing band pass filtered data and (c) showing AP1 picker characteristic function. Red inserts indicate the initial observed picks. (For interpretation of the references to color in this figure legend, the reader is referred to the web version of this article.)

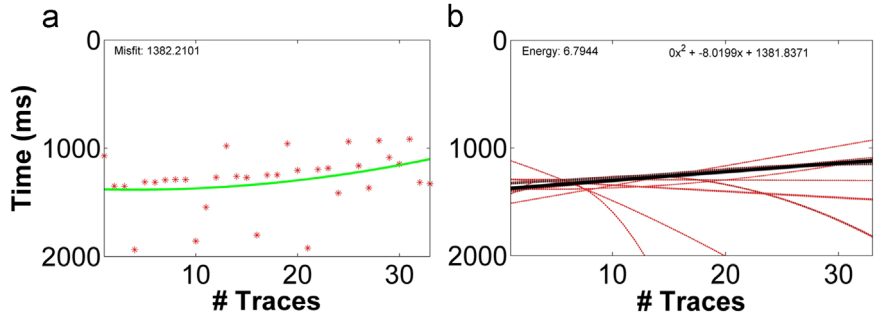

Fig. 6. (a) Initial fit before evolutionary search and (b) final search results [black] after iterative optimization of cost function for primary detection.

Table 1
Design parameters for AP1 & AP2 workflows used in this study. For additional details on parameter selection for AP1, refer Maity et al. (2014).

Parameter	Value
AP1: Attributes for training	a_1, a_2, a_3, a_4
AP1: Evaluation window, N	0.05 s
AP1: Trigger threshold for event declaration using CF	0.3
AP2: No. of traces for density measure, N_t	8
AP2: Evaluation window for density measure, win	0.2 s
AP2: Evolutionary Algorithm (EA), No. of generations	200
AP1: Δt for good picks (Eq. (3))	0.5 s

applied to this data subset and the workflow detects both primary and secondary arrivals for the four sample events shown. Fig. 12 shows the detections and highlights the robustness of the automatic event detection routine under relatively low signal-to-noise ratio conditions. We note that in all of the four examples shown, the primary detection is a late period S phase energy arrival while the secondary detection is the first break or possibly P phase arrival. This is expected in borehole environments where S wave is typically the most energetic and shows more strongly on the gathers.

For event gathers with propagation artifacts, the devised detection strategy iteratively moves towards the actual arrival based on a limited number of accurate phase detections clustered along the gather. This is highlighted with the plot of the updates observed during evolutionary search for two such sample events (Fig. 13).

The results obtained with this workflow (AP2) were compared with the original picks made using the AP1 algorithm as well as two other contemporary event picking algorithms (FilterPicker and MIMO). For reference, the parameters used for these algorithms have been specified under Tables 2 and 3. We need to highlight that the choice of most of these parameters is influenced by the data being processed and will vary based on factors ranging from dominant period of seismic wave-train to the sampling rate. For detailed understanding of these parameters, we suggest a review of the associated references.

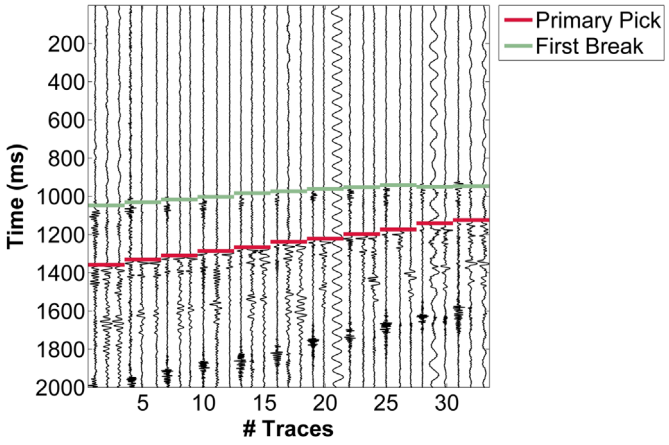

Fig. 8. Primary and secondary (first break) arrivals for reference event showing more robust primary arrival compared to the secondary detection.

For comparative analysis, manual picks were made (both P and S phase arrivals) for the entire data subset under study. Then, the offset of picks from each algorithm was compared with the baseline manual pick. This was done for all picks made provided a corresponding manual pick was available for comparison. The total picks possible for each event gather is 66 (33P phase picks+33S phase picks) giving us potentially 660P phase picks and 660S phase picks for analysis. Since all picks could not be identified manually with desired accuracy, the actual number of picks compared was considerably lower (more so for P phase arrivals). Fig. 14 shows examples of both very high and very low SNR event and the results from the picking routines used in the study. We observe the proposed workflow to perform reasonably well even in situations where the contemporary routines fail to make a usable pick or make erroneous arrival detections (Fig. 14c).

With the hybrid detection workflow (AP2), both primary and secondary picks are assigned if the algorithm is able to successfully detect them. However, this may not always be the case, in particular where we have relatively low signal-to-noise ratios.

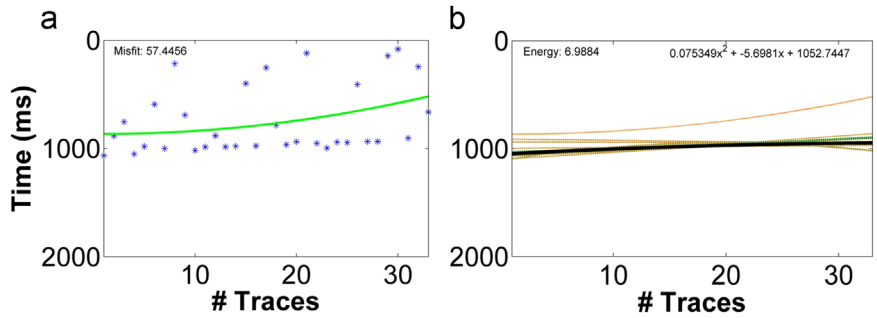

Fig. 7. (a) Initial fit over segmented data before evolutionary search and (b) final search results [black] after iterative optimization of cost function for secondary detection.

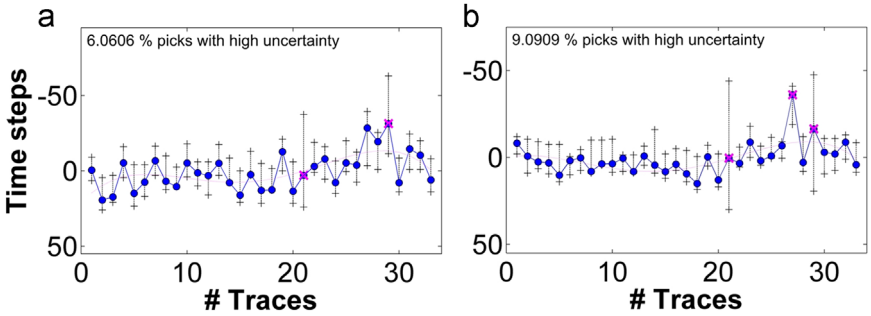

Fig. 9. Pick uncertainty estimates with blue dots showing the mean of the spread and the vertical bars showing the spread of uncertainty. Plot (a) shows pick uncertainty estimates for primary pick and (b) shows uncertainty estimates for secondary pick. Picks with relatively high uncertainty are tagged with a cross. (For interpretation of the references to color in this figure legend, the reader is referred to the web version of this article.)

Fig. 15 shows the total P and S phase detections made by the four methods and how they compare with total number of manual picks available.

We can clearly observe that in both cases, we were unable to pick most of the potential phase arrivals. This problem was particularly acute with P phase where the arrival energies were approximately 2 orders of magnitude lower than for S phase. Of the 660 potential picks for each phase, 20 had to be discarded as they correspond with vertical component (instrument noise issue) for geophone # 7. A total of 541S phase and 329P phase manual picks were successfully made. We observe that the proposed hybrid workflow (AP2) shows good results at offsets higher than $\sim$13 ms for P phase and $\sim$11 ms for S phase data. We also observe that the proposed algorithm is able to resolve almost all S phase arrivals that could be manually picked within $\pm$25 ms. However, we do not observe the same with P phase arrivals for many instances where the algorithm failed to pick due to lack of "preliminary" detections available for fitting. However, we do observe the results to show an overall improvement in arrival detectability albeit with higher uncertainty. This is further highlighted in Fig. 16 where the higher variances in the distribution of time offsets from picks made using AP2 algorithm points towards this uncertainty.

We also note that there are many instances where manual picks could not be made but the proposed workflow is able to detect a potential phase arrival. This could be true for some instruments (partial gather) as observed in Fig. 13 or across the entire gather. Fig. 17 shows a sample event where it is very hard to manually pick P phase onsets but the auto detection workflow is able to identify a possible P phase arrival.

Finally, we would like to highlight the demonstrated immunity towards noise from using AP2 algorithm. AS observed, this is primarily true for situations where atleast some picks can be initially made across the seismic gather. This is a necessary condition for the processing workflow to function as it then provides enough data for the cost function (Eq. (4)) to generate usable results and in the absence of which, the optimization methodology will fail. This implies that the effectiveness of this approach will be significantly dependent on the initial picking routine used for analysis (AP1 in this study). The better the algorithms used for the initial picks, the better the final AP2 results upon application of this workflow. So in situations where the signal-to-noise ratio is very low and initial picks cannot be made, the AP2 algorithm will not be able to provide usable picks. The value of this workflow lies in getting additional data in form of arrivals from catalogs where the signal quality is poor and significant arrivals though detectable need to be discarded due to insufficient coherence across the seismic

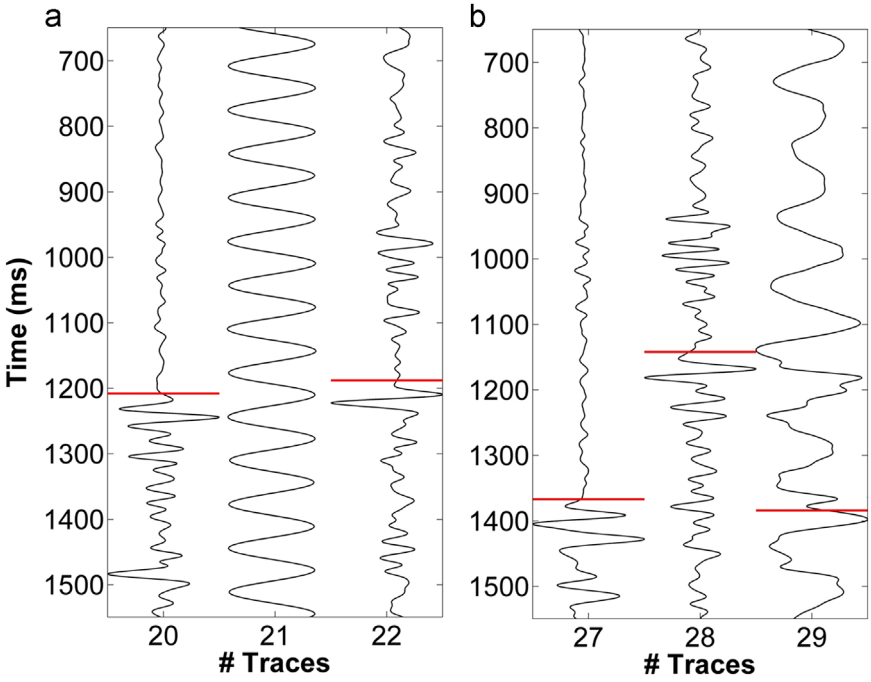

Fig. 10. Blow up sections showing trace # 21, 27 and 29 highlighting high uncertainty in S phase (trace # 21 & 29) and P phase (trace # 21, 27 and 29) arrivals.

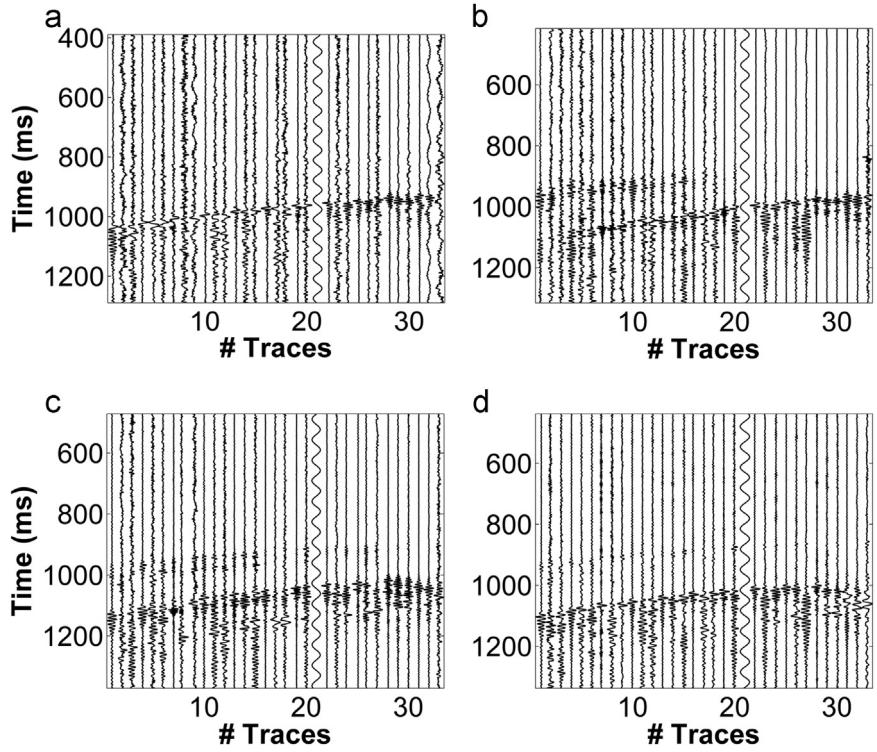

Fig. 11. Four sample events showing arrivals of both P and S phase energy. For subplots (a) and (d), P phase energy onset is very hard to detect. For subplots (b) and (c), the acquisition geometry leads to partial moveouts for P phase energy onset.

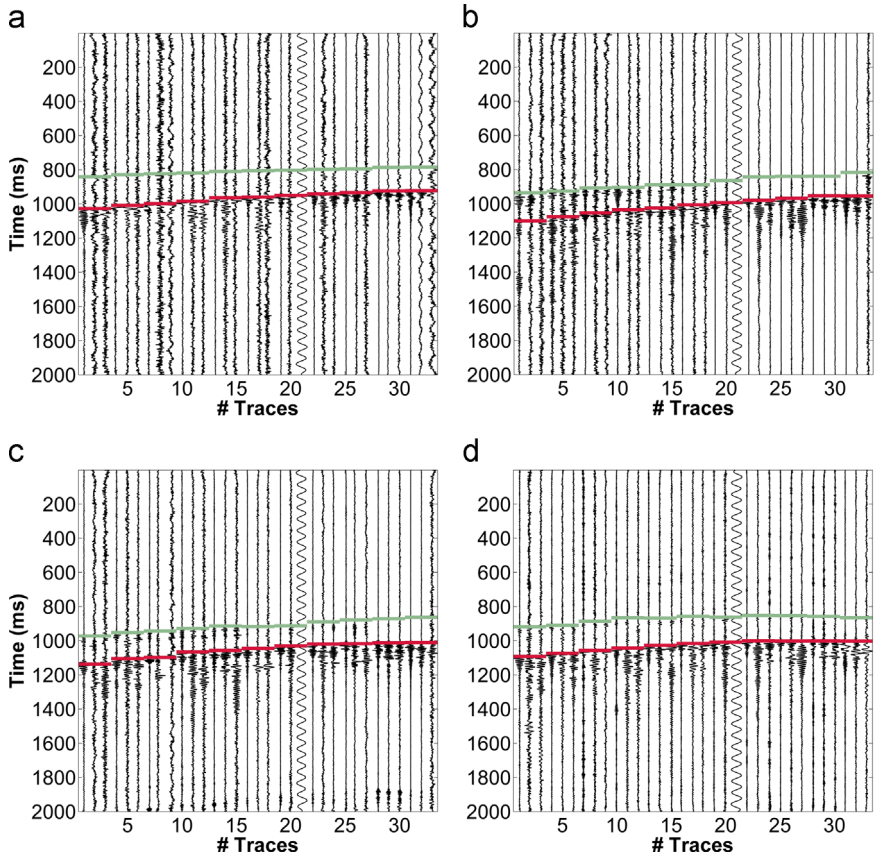

Fig. 12. Final phase detections for four selected events showing both primary and secondary detection. The algorithm works in situations where propagation geometry creates lower energy onsets for sections of the event gather (subplots b and c) or where attenuation leads to lower P phase onset energies (subplots a and d).

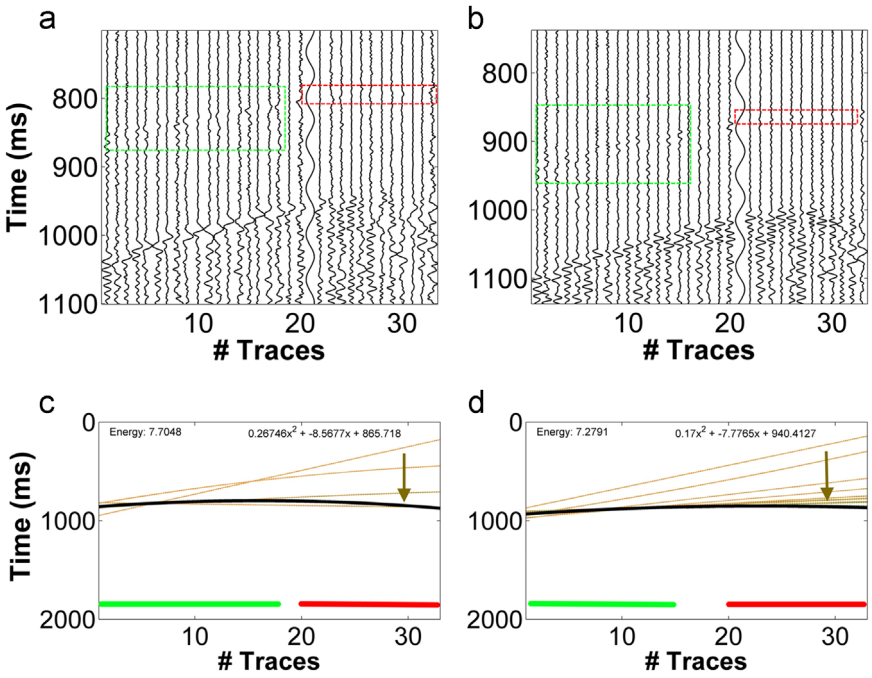

Fig. 13. Two sample iterative optimization runs with final event detection (black inserts) shown as subplots (c) and (d) as they correspond with arrivals shown in subplots (a) and (b). The green section highlights zone with relatively accurate preliminary detections based on AP1 and red inserts show sections of gather with relatively poor fit or no AP1 derived picks. The arrows highlight the direction of best fit with succesive iterations of evolutionary algorithm. (For interpretation of the references to color in this figure legend, the reader is referred to the web version of this article.)

Table 2
Design parameters for MIMO (event detection) algorithm used in this study. For additional details on parameter selection and other relevant parameters (association, phase picking), refer MIMO Reference Manual (2012).

Parameter	Value
Duration of STA-window	0.01 s
Duration of LTA-window	0.2 s
Detection threshold	2
Noise threshold	1
Typical duration of events	0.2 s
Filter type	Error prediction
Order of Butterworth bandpass filter	2
Low frequency	10 Hz
High frequency	90 Hz
Duration of noise window	0.1 s

Table 3
Design parameters for FilterPicker routine used in this study. For additional details on parameter selection, refer Lomax et al. (2012).

Parameter	Description	Value
T_{filter}	Long period for filtered signals	0.25 s
T_{long}	Time over which time averaged statistics are computed	2 s
S_1	Trigger threshold for event declaration using CF	10
S_2	Pick is declared if within T_{up} after trigger, CF exceeds $S_2 \times T_{\text{up}}$	10
T_{up}	Time window for pick validation	0.1 s

gathers.

5. Conclusion

A robust event detection routine has been developed which utilizes expected moveout characteristics for downhole sensor deployments to identify potential events from raw microseismic datasets. The workflow also searches for secondary phases if

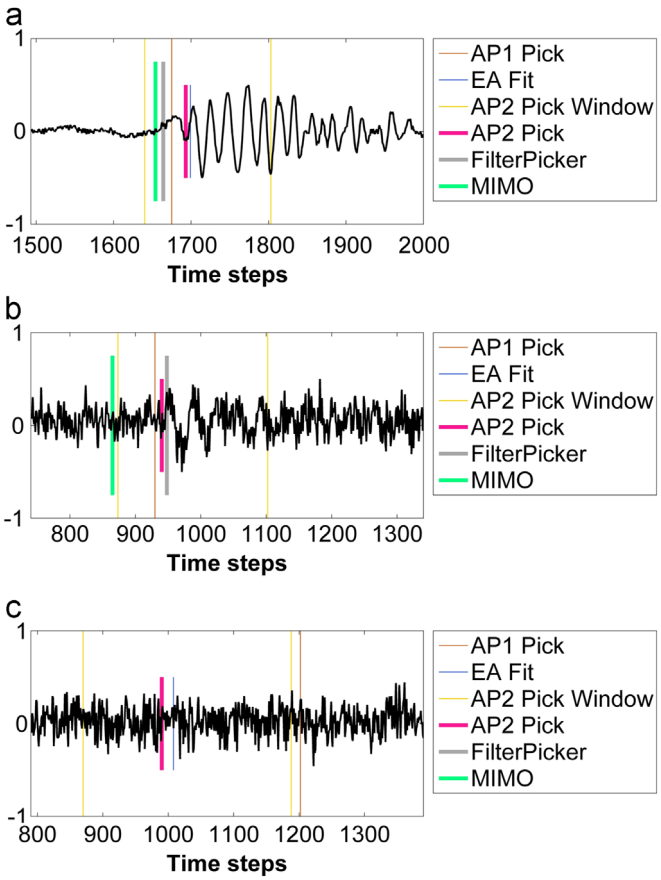

Fig. 14. Sample trace blow out sections highlighting energy at arrivals and corresponding picks made by algorithms under study for (a) high signal-to-noise, (b) moderate signal-to-noise and (c) very low signal-to-noise test cases.

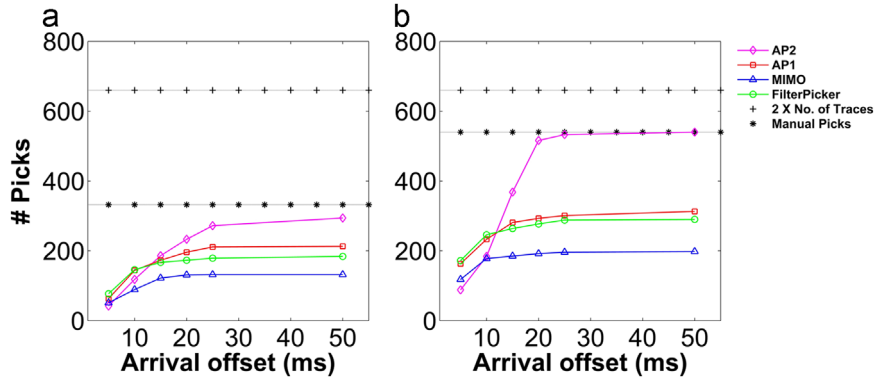

Fig. 15. Results from comparative analysis of four picking algorithms. Subplot (a) shows results for P phase detections and (b) shows results for S phase detections.

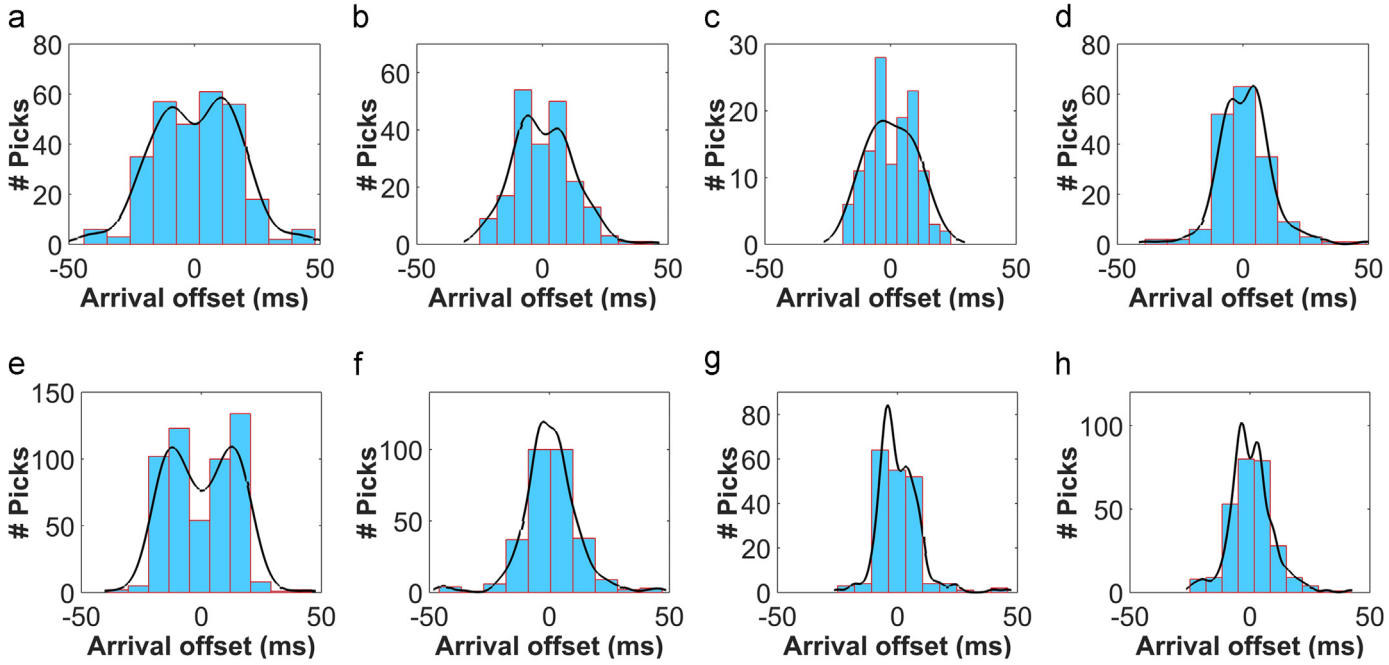

Fig. 16. Distribution of time differences between automated and manual picks for P phase arrivals using (a) AP2, (b) AP1, (c) MIMO and (d) FilterPicker algorithms and for S phase arrivals using (e) AP2, (f) AP1, (g) MIMO and (h) FilterPicker algorithms.

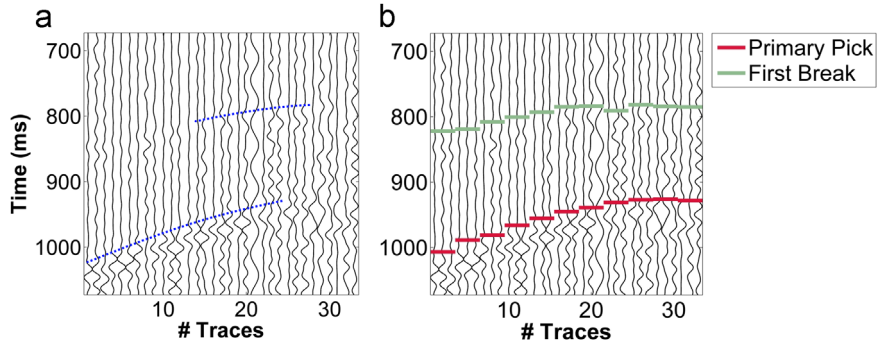

Fig. 17. Subplot (a) shows time window with a possible event and subplot (b) shows final primary and secondary detections using AP2. Blue dotted inserts show possible P & S arrival as per visual inspection but it is clear that manual picking is extremely hard due to very low signal-to-noise ratio. (For interpretation of the references to color in this figure legend, the reader is referred to the web version of this article.)

possible to isolate potential P and S phase energy arrivals in the data. Our tests on application with real microseismic monitoring data from the Marcellus shows very good applicability and improved detectability when compared with contemporary event detection algorithms in use. While we have used a neural-nets based hybrid autopicker to make the initial picks, the workflow allows flexibility to use any other primary picking algorithm to make these initial pick estimates, provided the picks are reasonably accurate. While the proposed workflow shows relatively high immunity towards incoherent background noise, directional coherent noise artifacts can cause significant misclassifications. In order to tide over this issue, we propose the use of this

microseismic event detection algorithm with a robust noise removal tool such as time-delay or adaptive beamformer (Widrow and Sterns, 1985) which can remove coherent noise in a robust manner before the actual detection routine is applied. Future work involves testing the efficacy of such a modified workflow including adaptive noise filtering for downhole microseismic applications by studying the impact of the same on quality of identified microseismic source parameters.

Acknowledgement

This work was supported by RPSEA Project no. 11122-20. We also acknowledge WPX Energy for providing access to active hydraulically fractured wells of opportunity in Marcellus shale play and Halliburton for acquiring the microseismic data used in this study. Finally, we would like to acknowledge Jordan Ciezobka from GTI for valuable suggestions to improve this work.

References

Allen, R.V., 1978. Automatic earthquake recognition and timing from single traces. Bull. Seismol. Soc. Am. 68, 1521–1532.

Chen, Z., 2005. A multi-window algorithm for automatic picking of microseismic events on 3-C data. In: 75th SEG Annual Meeting & Exhibition, Houston, TX, 6–11 November. doi:10.1190/1.2147921.

Fischer, T., Bouskova, A., Eisner, L., Calvez, J.L., 2007. Automated P- and S-wave picking of micro earthquakes recorded by a vertical array. In: Proceedings of the 69th EAGE Conference & Exhibition, London, UK, 11–14 June.

Kurzon, I., Vernon, F.L., Rosenberger, A., Ben-Zion, Y., 2014. Real-time automatic detectors of P and S waves using singular value decomposition. Bull. Seismol. Soc. Am. 104 (4), 1696–1708. http://dx.doi.org/10.1785/0120130295.

Lomax, A., Satriano, C., Vassallo, M., 2012. Automatic picker developments and optimization: FilterPicker – a robust, broadband picker for real-time seismic monitoring and earthquake early warning. Seismol. Res. Lett. 83 (3), 531–540. http://dx.doi.org/10.1785/gssrl.83.3.531.

Maity, D., Aminzadeh, F., Karrenbach, M., 2014. Novel hybrid artificial neural network based autopicking workflow for passive seismic data. Geophys. Prospect. 62, 834–847. http://dx.doi.org/10.1111/1365-2478.12125.

MIMO Reference Manual, 2012. NORSAR, Kjeller, Norway, p. 90.

Oye, V., Roth, M., 2003. Automatic seismic event location for hydrocarbon reservoirs. Comput. Geosci. 29, 851–863. http://dx.doi.org/10.1016/S0098-3004(03)00088-8.

Saragiotis, C.D., Hadjileontiadis, L.J., Panas, S.M., 2002. PAI-S/K: a robust automatic seismic P phase arrival identification scheme. IEEE Trans. Geosci. Remote Sens. 40 (6), 1395–1404. http://dx.doi.org/10.1109/TGRS.2002.800438.

Song, F., Kuleli, H.S., Toksöz, M.N., Ay, E., Zhang, H., 2010. An improved method for hydrofracture-induced microseismic event detection and phase picking. Geophysics 75 (6), A47–A52. http://dx.doi.org/10.1190/1.3484716.

Widrow, B., Sterns, S.D., 1985. Adaptive Signal Processing. Prentice-Hall, Englewood Cliffs, NJ, ISBN: 9780130040299.

Wu, S., Yamada, M., Tamaribuchi, K., Beck, J.L., 2015. Multi-events earthquake early warning algorithm using a Bayesian approach. Geophys. J. Int. 200 (2), 789–806. http://dx.doi.org/10.1093/gji/ggu437.